



**HAL**  
open science

## Rheological properties of synthetic mucus for airway clearance

Olivier Lafforgue, Isabelle Seyssiecq, Sébastien Poncet, Julien Favier

► **To cite this version:**

Olivier Lafforgue, Isabelle Seyssiecq, Sébastien Poncet, Julien Favier. Rheological properties of synthetic mucus for airway clearance. *Journal of Biomedical Materials Research Part A*, 2018, 106 (2), pp.386 - 396. 10.1002/jbm.a.36251 . hal-01678912

**HAL Id: hal-01678912**

**<https://hal.science/hal-01678912>**

Submitted on 4 May 2018

**HAL** is a multi-disciplinary open access archive for the deposit and dissemination of scientific research documents, whether they are published or not. The documents may come from teaching and research institutions in France or abroad, or from public or private research centers.

L'archive ouverte pluridisciplinaire **HAL**, est destinée au dépôt et à la diffusion de documents scientifiques de niveau recherche, publiés ou non, émanant des établissements d'enseignement et de recherche français ou étrangers, des laboratoires publics ou privés.

1  
2  
3 **Rheological properties of synthetic mucus for airway clearance**

4 O. Lafforgue<sup>1</sup>, I. Seyssiecq<sup>1</sup>, S. Poncet<sup>1,2</sup>, J. Favier<sup>1</sup>

5  
6 <sup>1</sup>*Aix-Marseille Université, CNRS, Ecole Centrale de Marseille, Laboratoire M2P2 UMR 7340*  
7  
8 *38 rue F. Joliot-Curie, Technopôle de Château-Gombert, 13451 Marseille, France*

9  
10 <sup>2</sup>*Université de Sherbrooke, Faculté de génie, Département de génie mécanique*  
11  
12 *2500 Boulevard de l'Université, Sherbrooke (QC) J1K 2R1, Canada*

13  
14 ABSTRACT: In this work, a complete rheological characterization of bronchial mucus  
15 simulants based on the composition proposed by Zahm et al. [1] is presented. Dynamic Small  
16 Amplitude Oscillatory Shear (SAOS) experiments, Steady State (SS) flow measurements and  
17 three Intervals Thixotropy Tests (3ITT), are carried out to investigate the global rheological  
18 complexities of simulants (viscoelasticity, viscoplasticity, shear - thinning and thixotropy) as  
19 a function of scleroglucan concentrations (0.5 to 2wt%) and under temperatures of 20 and 37  
20 °C. SAOS measurements show that the limit of the linear viscoelastic range as well as the  
21 elasticity both increase with increasing scleroglucan concentrations. Depending on the  
22 sollicitation frequency, the 0.5wt% gel response is either liquid-like or solid-like, whereas  
23 more concentrated gels show a solid-like response over the whole frequency range. The  
24 temperature dependence of gels response is negligible in the 20-37°C range. The Herschel-  
25 Bulkley (HB) model is chosen to fit the SS flow curve of simulants. The evolution of HB  
26 parameters versus polymer concentration show that both shear-thinning and viscoplasticity  
27 increase with increasing concentrations. 3ITTs allow calculation of recovery thixotropic times  
28 after shearings at 100s<sup>-1</sup> or 1.6s<sup>-1</sup>. Empiric correlations are proposed to quantify the effect of  
29 polymer concentration on rheological parameters of mucus simulants.  
30  
31  
32  
33  
34  
35  
36  
37  
38  
39  
40  
41  
42  
43  
44  
45  
46  
47  
48  
49

50  
51 KEYWORDS: synthetic bronchial mucus; viscoelasticity, viscoplasticity, shear - thinning,  
52 thixotropy  
53  
54  
55  
56  
57

## INTRODUCTION

A large number of fluids in human body, such as blood or mucus, produced by different organs, are known to exhibit complex non Newtonian rheological properties under physiological states. When transported in the airways as a result of cough or cilia beating, bronchial mucus is characterized by a non constant, shear rate and time dependent viscosity, in both normal and pathological conditions. Bronchial mucus is mainly composed of water (90-95%), mucins (2-5%), lipids (1-2%), salts (1%), 0.02% of DNA and other molecules such as cells debris [2]. Mucins are high molecular weight glycoproteins insuring a structural protection function. The entangled and cross-linked network of its branched chains forms a 3D matrix spanning the mucus gel layer [3]. As a consequence of this complex internal structure, bronchial mucus is a non Newtonian fluid displaying all the possible rheological complexities such as viscoplasticity, shear-thinning, viscoelasticity and thixotropy. All these properties directly affect the way mucus flows and, as a consequence, the vital clearance function of the mucus layer coating the airways. The mechanism of mucus clearance can be described by the following two steps:

Step 1: inhaled particles or pathogens are trapped inside the mucus gel where enzymes and antibodies can biochemically disrupt them.

Step 2 : mucus is mainly transported by the mucociliary mechanism or by cough towards the pharynx where it is either expectorated or digested.

It is however known that, under certain disease conditions such as Cystic Fibrosis (CF), the clearance function is affected by modifications of the mucus composition and consequently, of its viscosity. Due to a lack of hydration (in the case of CF), mucus can indeed become very thick and difficulties may arise to properly evacuate this fluid from the airways where it can accumulate and become more easily infected. A good understanding of mucus rheology is

1  
2  
3 thus of prime importance in order to develop new care solutions for patients suffering from  
4  
5 CF or other chronic respiratory diseases. Among possible care solutions, clearance helping  
6  
7 devices, based on different technologies, have been developed during the last decades. These  
8  
9 small devices can be used by patients at home, on a daily basis to increase the volume of  
10  
11 mucus expectoration and limit the need for respiratory physiotherapy. As an example, a newly  
12  
13 developed apparatus known as the Simeox®, imposes an oscillatory air depression to the air  
14  
15 flow during the exhalation phase of the patient. Based on the thixotropic and shear-thinning  
16  
17 nature of mucus, such a solicitation induces a decrease of its viscosity and stimulates its  
18  
19 expectoration. More insight into the rheology of respiratory mucus is needed to further  
20  
21 improve the efficiency of such clearance helping devices. Although there is a large number of  
22  
23 studies devoted to the rheological characterization of certain types of mucus, the results are  
24  
25 still difficult to interpret, due to the use of different rheological techniques, but also due to the  
26  
27 time evolution (aging) of such biological materials [4]. Furthermore, variations in the method  
28  
29 used to collect samples (contamination issues), together with the natural variability  
30  
31 (depending on the patient, the pathology, the occurrence of an infection...) of this complex  
32  
33 biological fluid lead to important discrepancies in the existing literature, concerning the  
34  
35 results on mucus rheological characterization [5]. Numerous previous works devoted to the  
36  
37 study of mucus rheology (either synthetic or native mucus from different organs), have only  
38  
39 described part of its rheological properties. For instance, many works have used dynamic  
40  
41 oscillatory shear measurements to characterize mucus rheology [6 ; 7 ; 8 ; 9; 10 ; 11 ; 12].  
42  
43 Under small deformations (SAOS) these measurements mostly reflect the properties of mucus  
44  
45 under its native, unperturbed state and are useful to describe the linear viscoelastic response of  
46  
47 mucus. On the contrary, in other works, the authors have made the choice to characterize  
48  
49 mucus rheology using only continuous shear experiments [1 ; 13 ; 14; 15]. In these cases, the  
50  
51 measured properties mostly reflect the flow behavior of mucus and can be used to investigate  
52  
53  
54  
55  
56  
57  
58  
59  
60

1  
2  
3 its viscosity under physiological shearing rates prevailing in human lungs during normal  
4 functioning or during temporary events such as cough. Even in studies where both dynamic  
5 oscillatory and shear flow measurements were carried out, the thixotropic nature of mucus  
6 was not accounted for [5; 16 ; 17 ; 18 ; 19; 20 ; 21], or at least not on a quantitative point of  
7 view [22 ; 23 ; 24]. As a consequence, a complete and intrinsically consistent characterization  
8 campaign is still missing in the open literature. As the use of real mucus implies strong issues  
9 related to available quantities, and rises questions about the impact of the collection method  
10 on the fluid composition, the choice made in this work is to use mucus simulants. In this  
11 context, this work proposes a rheological characterization of mucus simulants at different  
12 active polymer concentrations (0.5 to 2%), under a temperature of 20 or 37°C allowing to  
13 cover the range of air physiological temperature along the airways and using a broad range of  
14 available rheological tests (SAOS, controlled shear stress SS flow tests and 3ITT). In an  
15 attempt to quantify the measured properties, empirical equations are used to represent the  
16 evolution of different rheological parameters as a function of the active polymer  
17 concentration.

## 38 **MATERIALS AND METHODS**

### 39 **Preparation of mucus simulants**

40  
41 The composition and preparation of polymeric synthetic solutions used to mimic human  
42 bronchial mucus are described in Zahm *et al.* [1]. To account for the natural variability of real  
43 mucus from one patient to another but also depending on health conditions, gels with different  
44 scleroglucan (Actigum™) concentrations ranging from 0.5 to 2wt% were prepared. Mucus  
45 simulants are aqueous solutions mainly composed of two types of polymers, Viscogum™ FA  
46 (Cargill™) and Actigum™ CS 6 (Cargill™). The polymers used in this work were kindly  
47 provided by the Laserson compagny (Etampes, France). Viscogum™ FA is a galactomannan  
48  
49  
50  
51  
52  
53  
54  
55  
56  
57

1  
2  
3 gum extracted from locust beans and Actigum™ CS 6 is a scleroglucan (branched  
4  
5 homopolysaccharide). It consists in a glucose chain branched every three units by an  
6  
7 additional glucose forming a three dimensional (triple helix) structure. Sodium chloride  
8  
9 (99.8+% NaCl) and di-sodium tetraborate 10aq (99.5+% Na<sub>2</sub>B<sub>4</sub>O<sub>7</sub>·10H<sub>2</sub>O) were purchased  
10  
11 from Chem-Lab NV (Zedelgem, Belgium). Distilled water used in all preparations was  
12  
13 produced using a 2012 distillator (GFL, France). Mucus simulants solutions were prepared  
14  
15 within glass bottles filled with 200 mg of distilled water. Then, 0.9wt% of NaCl, 0.5wt% of  
16  
17 Viscogum™ FA and a chosen fraction (ranging from 0.5wt% to 2wt%) of Actigum™ CS 6  
18  
19 were successively added into the solution under magnetic stirring (Ikamag® RET) at room  
20  
21 temperature. The mixture was kept under agitation for 48h at room temperature. After this  
22  
23 time period, a mass corresponding to 4mL of di-sodium tetraborate at 0.02M was added. This  
24  
25 addition induces the cross-linking of the polymeric chains, building a 3D gel matrix that  
26  
27 mimicks the mucin network responsible for the internal structure of real mucus. The agitation  
28  
29 is kept for a few more hours before storing the final mixture at 4°C. Before performing the  
30  
31 measurements, the solution is fractionnated into several 30mL plastic vials and then allowed  
32  
33 to recover at room temperature. Such mucus simulants were found to mimic accurately the  
34  
35 main properties of bronchial mucus in the case of different pathologies.  
36  
37  
38  
39  
40

## 41 **Rheological measurements**

### 42 *Rheometers and measuring systems*

43  
44  
45 Rheological measurements were performed using two controlled-stress rheometers, the AR  
46  
47 550 and the DHR-2 (TA Instruments) equipped with a measuring system consisting of a 2°  
48  
49 stainless steel cone (40 mm or 50 mm in diameter). The temperature was controlled by a  
50  
51 Peltier plate. A wet steel lid or a thin silicone oil layer insuring a water saturated atmosphere  
52  
53 around the sample was used as a dehydration preventing solution.  
54  
55  
56  
57

1  
2  
3 ***Sample loading***  
4

5 A small amount of gel was loaded onto the Peltier plate by gently pouring it from the vial in  
6 order to minimize shear history effects. The geometry was then lowered down to the  
7 corresponding gap plus a few micrometers and the excess of fluid was removed on the edges,  
8 the exact gap value was then set. The desired temperature (20 °C or 37°C) was also set before  
9 the tests began.  
10  
11  
12  
13  
14  
15

16  
17 ***Measurements protocols***  
18

19 Viscoelastic properties of the simulants were investigated through a series of dynamic shear  
20 experiments (Small Amplitude Oscillatory Shear: SAOS). The results were interpreted based  
21 on the evolution of the elastic and viscous moduli ( $G'$ ,  $G''$ ) and the loss angle ( $\delta$ ) as a function  
22 of the sinusoidal input. The stress dependency of the different gels (0.5wt% to 2wt% in active  
23 polymer) response was first measured via stress amplitude sweeps at constant frequency  
24 ( $\frac{1}{2\pi}$  Hz). This is a classical test carried out in order to determine, for each solution, the limit  
25 of the Linear ViscoElastic (LVE) range. The frequency dependency (in a maximum range of  
26  $10^{-5}$  to 100 Hz) of the different gels response was also measured at constant stress amplitude,  
27 within the LVE range according to the stress amplitude sweep results. The temperature  
28 dependency of simulants rheological properties was finally investigated by comparing stress  
29 amplitude sweeps obtained for a given sample at either 20°C (ambient air temperature) or  
30 37°C (physiological temperature in the lower airways). However, to fully characterize the  
31 behavior of a mucus layer in response to in vivo solicitations such as cough or air flows  
32 artificially induced by clearance helping devices, the rheological measurements have to be  
33 performed far beyond the LVE range. Rotational controlled shear stress flow tests were then  
34 used to determine the rheological properties of the mucus simulants under shear flow  
35 conditions. In order to quantify the viscoplastic and the shear-thinning effects independently  
36  
37  
38  
39  
40  
41  
42  
43  
44  
45  
46  
47  
48  
49  
50  
51  
52  
53  
54  
55  
56  
57  
58  
59  
60

1  
2  
3 of the thixotropic ones, steady state rheograms were recorded. Such a steady state curve is  
4  
5 obtained by applying a given shear stress until the corresponding shear rate reaches a constant  
6  
7 value. Steady state (SS) flow curves of the different simulants were modeled using a 3  
8  
9 parameters Herschel-Bulkley (HB) model. This model accounts for the fluid viscoplasticity  
10  
11 via the yield stress value ( $\tau_{0HB}$ ) and for its shear - thinning behavior via the flow (n) and  
12  
13 consistency (K) indexes values. The thixotropy of the more concentrated mucus simulant was  
14  
15 separately quantified using three Intervals Thixotropy Tests (3ITT). A 3ITT test consists in a  
16  
17 stepwise change of stress or strain rate to successively monitor the initial structure, then its  
18  
19 breaking up and finally its recovery. More precisely, the 3ITTs applied here can be described  
20  
21 as follows:  
22  
23

24  
25  
26 First interval: the sample is submitted to very low shear conditions ( $\dot{\gamma} = 0.029s^{-1}$ ). This  
27  
28 interval gives a reference for the fluid structure "at rest" or at least under very low shear.  
29  
30

31  
32 Second interval: higher shear conditions are imposed by applying a constant shear stress or  
33  
34 shear rate to disrupt the internal structure until a steady state is reached (depending on the  
35  
36 chosen stress or strain rate value). In our case, a constant shear rate value of either  $1.6s^{-1}$  or  
37  
38  $100s^{-1}$  was applied during step 2, in order to submit the sample to shearing conditions  
39  
40 representative of either normal shearing conditions in the airways, or during peculiar events  
41  
42 such as cough.  
43  
44

45  
46 Third interval: the sample is allowed to recover under very low shear conditions again  
47  
48 ( $\dot{\gamma} = 0.029s^{-1}$ ). A time scale characterizing a given state of regeneration (chosen here at 90%  
49  
50 and 100% of recovery based on the initial structure measured during step 1.) can then be  
51  
52 calculated.  
53  
54  
55  
56  
57

## RESULTS

### SAOS tests

Stress amplitude and frequency sweep tests conducted at a constant temperature of 20°C, on simulant gels at different Actigum™ concentrations, all display the same feature. An example is given in figure 1 for a 1.5wt% Actigum™ gel (figure 1 (a) stress amplitude sweep, (b) frequency sweep). A value of the elastic modulus  $G'$  above the viscous modulus  $G''$  implies that the elastic behavior dominates the viscous one and indicates a solid-like or gel-like behavior, while  $G'' > G'$  indicates a liquid-like behavior. In figure 1 (a), the stress amplitude value for which the transition from one behavior to the other is observed, is denoted by  $\tau_f$  (flow point value corresponding to the crossover of moduli  $G' = G''$ ,  $\tan(\delta) = 1$ ) and will be discussed hereafter. As a consequence, in the case of figure 1.(b) for which  $\tau = 1 \text{ Pa} < \tau_f$ , the mucus simulant shows a gel-like behavior for all frequencies ranging from  $10^{-3}$  to 10 Hz. In the case of figure 1.(a), under a constant frequency of  $\frac{1}{2\pi} \text{ Hz}$ , the two domains are successively observed, with a solid-like behavior for  $\tau < \tau_f$ , then liquid-like behavior for  $\tau > \tau_f$ .

### *Stress amplitude sweep tests*

The stress amplitude dependency of the different gels response was recorded via stress amplitude sweeps at a constant frequency ( $\frac{1}{2\pi} \text{ Hz}$ ) for all the concentrations in active polymer (0.5wt% to 2wt%). The results obtained are displayed in figure 2.

For all polymer concentrations, a plateau region for  $G'$  and  $G''$  moduli defines the LVE Range at the preset frequency. A yield stress value ( $\tau_y$ ) limits the LVE range and is determined from the end of the moduli plateau. Since the  $G'$  curve often deviates first from the plateau, the  $G'$

1  
2  
3 function is commonly chosen to determine  $\tau_y$ . Here, a 10% deviation from the plateau has  
4  
5 arbitrarily been set for  $\tau_y$  calculations . The yield stress is the stress limit below which no  
6  
7 significant change of the internal structure occurs. For  $\tau < \tau_y$  the sample is displaying  
8  
9 reversible viscoelastic behavior. On the contrary, above  $\tau_y$ , the measurements no longer  
10  
11 reflect the structure at rest due to early signs of stress induced microstructural evolutions.  
12  
13 Based on the value of the yield stress and of the corresponding critical deformation  $\gamma_c$ , one can  
14  
15 also calculate the volumetric energy of cohesion of the 3D network  $E_c$  in  $J.m^{-3}$  (eq. (1)) [25].  
16  
17 This energy of cohesion can be used in a quantitative manner as a measure of the extent of  
18  
19 intermolecular and intramolecular interactions of the polymeric internal structure [26].  
20  
21  
22  
23

$$E_c = \frac{1}{2} \tau_y \cdot \gamma_c \quad (1)$$

24  
25  
26  
27  
28 In the case of the mucus simulants tested here, it can be seen in figure 2 that above the critical  
29  
30 yield stress,  $G'$  decreases while  $G''$  shows an overshoot before decreasing. This kind of  
31  
32 behavior has been observed on lots of gels by Mezger [27] and is classified as a "Type III  
33  
34 behavior or weak strain overshoot" by Hyun et al [28]. The flow point ( $\tau_f$ ) is identified as the  
35  
36 stress value for which a moduli crossover ( $G'=G''$ ,  $\tan(\delta)=1$ ) is observed. This flow point  
37  
38 corresponds to the stress above which the material becomes more viscous than elastic due to  
39  
40 critical microstructural breakdowns. Finally the stress corresponding to the maximum of  $G''$   
41  
42 (peak overshoot) is denote by  $\tau_{peak}$  and is, for all concentrations, almost superimposed to the  
43  
44 flow point stress (except for the 0.5wt% gel for which the  $G''$  overshoot does not appear). The  
45  
46 range between  $\tau_y$  and  $\tau_f$  is sometimes referred as the "yield zone" or the "yield / flow  
47  
48 transition range" [27]. In this range, despite the predominance of elastic behavior ( $G' > G''$ ),  
49  
50 irreversible deformations might locally have already taken place.  
51  
52  
53  
54  
55  
56  
57  
58  
59  
60

1  
2  
3 In the case of mucus simulants studied here, G' and G'' moduli plateau values, as well as  
4 yield, flow and peak stresses and volumetric cohesive energy, all show increasing values  
5 according to the Actigum™ concentration as reported in table 1. The evolution with the  
6 Actigum™ concentration of the different transition stresses ( $\tau_y$ ,  $\tau_f$  and  $\tau_{peak}$ ) as well as the  
7 volumetric energy of cohesion ( $E_c$ ) and the plateau moduli values are all displayed in figure 3.  
8  
9

10  
11  
12  
13  
14 For quantification purposes, yield, flow and peak stresses variations with Actigum™  
15 concentration can be described by power law empirical relationships reported hereafter  
16 (equations 2 & 3). As previously mentioned, flow and peak stresses are almost superimposed,  
17 which makes sense since they both refer to the actual beginning of macroscopic flow of the  
18 gel ( $G'' > G'$  and friction starts decreasing). As a consequence a single empirical correlation is  
19 needed to account for the effect of polymer concentration on both flow and peak stresses.  
20  
21  
22  
23

24 Equation 2 gives the quantitative evolution of the yield stress ( $\tau_y$  in Pa) as a function of  
25 Actigum™ concentration (C in wt%):  
26  
27

$$\tau_y = 1.54 C^{2.31} \quad R^2 = 0.981 \quad (2)$$

28 Equation 3 accounts for the Actigum™ dependency of both  $\tau_f$  and  $\tau_{peak}$ :  
29  
30  
31

$$\tau_f \text{ \& } \tau_{peak} = 4.66 C^{1.68} \quad R^2 = 0.990 \quad (3)$$

32  
33  
34  
35  
36  
37 These evolutions are qualitatively compared to the evolution of the yield stress calculated  
38 from the HB modelling of the SS flow curve ( $\tau_{0HB}$ ) (see discussion part). Concerning G' and  
39 G'' plateau values (in Pa), they increase linearly (Figure 3(b)) with the active polymer  
40 concentration (in wt%) with an average slope of 10 for G'' and 49 for G'. The evolution of the  
41 volumetric energy of cohesion ( $E_c$  in  $J.m^{-3}$ ) of the 3D gel internal network versus the  
42 Actigum™ concentration (C in wt%) is also a power law as reported in equation 4:  
43  
44  
45  
46  
47  
48  
49  
50  
51  
52  
53  
54  
55  
56  
57

1  
2  
3  $E_c = 0.076 C^{1.95} \quad R^2 = 0.968$  (4)  
4  
5

6 ***Temperature dependence of the LVE range***  
7

8 The temperature dependence of the LVE range of mucus simulants was measured by  
9 comparing stress amplitude sweeps obtained at either 20°C (ambient temperature) or 37°C  
10 (physiological temperature in the lower airways). This temperature range was chosen in  
11 accordance to the possible range of variation for the air at different stages of respiratory  
12 airways. Figure 4 presents the variations of elastic modulus and viscous modulus versus the  
13 stress amplitude for a constant frequency ( $\frac{1}{2\pi}$  Hz) and a given Actigum™ concentration  
14 (0.75 wt%) at either 20°C or 37°C. Each curve is the average of 3 successive measurements.  
15 Measurements were also performed with simulants at different polymer concentrations and all  
16 display qualitatively identical results.  
17  
18  
19  
20  
21  
22  
23  
24  
25  
26  
27  
28  
29

30 As it is observed in figure 4, the LVE range of the mucus simulant gel as well as the different  
31 stresses ( $\tau_y$ ,  $\tau_f$ ,  $\tau_{peak}$ ) characterizing the solid - liquid transition zone show very little  
32 dependence on the temperature in the 20-37°C range. The curves obtained at either 20 or  
33 37°C are almost superimposed and the observed differences are of the same order of  
34 magnitude than reproducibility. Concerning the gels studied here, it can be concluded that the  
35 effect of temperature in the 20-37°C range on mucus simulants rheological properties is not  
36 significant compared to reproducibility.  
37  
38  
39  
40  
41  
42  
43  
44  
45  
46

47 ***Frequency sweep tests***  
48

49 Since the frequency is the inverse of a time, frequency sweep tests are usually performed in  
50 order to investigate the behavior of a substance as a function of the sollicitation characteristic  
51 time under small deformations. Short-term behavior of the sample is then simulated at high  
52 frequencies, whereas long-term behavior is displayed under low frequencies. The main  
53  
54  
55  
56  
57  
58  
59  
60

1  
2  
3 concern under very low frequencies is the conservation of the sample during the important  
4  
5 timelag needed to obtain these measuring points. So in these cases, a special care has to be  
6  
7 taken to control samples dehydration. The frequency dependence of the mucus simulants  
8  
9 response was measured by oscillating stress at increasing frequencies (maximum range:  $10^{-5}$  to  
10  
11 100 Hz) and a constant stress amplitude corresponding to a small deformation, i.e. within the  
12  
13 LVE range ( $\tau < \tau_y$ ) as measured at  $\frac{1}{2\pi}$  Hz (see table 1.). Figure 5 gathers the evolutions of  
14  
15 elastic modulus (a), viscous modulus (b) and loss angle (c) as a function of the applied  
16  
17 frequency for the different Actigum™ concentrations.

21  
22 Since working at very low frequencies implies a long experiment duration and, as a  
23  
24 consequence, a more important risk of sample dehydration, all the simulants have been  
25  
26 studied in the common range  $10^{-2}$  to 10 Hz. only in the case of the more diluted and the more  
27  
28 concentrated gels, the frequency range was enlarged to  $10^{-4}$  - 10 Hz and  $10^{-5}$  - 10 Hz to  
29  
30 investigate the possible occurrence of a low frequency moduli crossover. Over the whole range  
31  
32 of frequencies, simulants with Actigum™ concentrations ranging from 0.75wt% to 2wt%,  
33  
34 show a gel-like behavior characterized by an almost parallel low increase of  $G'$  and  $G''$  (in  
35  
36 log-log scale) with  $G'$  values 2 to 7 times higher than  $G''$ . Such a behavior is characteristic of a  
37  
38 soft gel in which intermolecular forces are mostly responsible for the 3D internal network  
39  
40 [27]. Therefore elastic behavior dominates the viscous one over the entire frequency range  
41  
42 attesting for the gel stability.  $G'$  and  $G''$  only show a slight frequency dependence displaying  
43  
44 an average slope in log-log representation of 0.1 in the case of  $G'$  and 0.04 in the case of  $G''$   
45  
46 (see discussion part for interpretation).  
47  
48  
49  
50

51  
52 The less concentrated simulant (0.5 wt%) displays a different behavior.  $G'$  and  $G''$  show a  
53  
54 more important frequency dependence, especially under low frequencies due to a more  
55  
56  
57

1  
2  
3 flexible network. A moduli crossover (characterized by  $\tan(\delta) = 1$  in figure 5 (c)) is also  
4  
5 observed at low frequencies ( $< 2 \cdot 10^{-3}$  Hz) for which  $G'' > G'$ . Such a behavior corresponds to  
6  
7 a liquid-like behavior and can be observed when a deformation (even very small) is applied at  
8  
9 a sufficiently low rate (i.e. during a long time). On the contrary, an identical deformation  
10  
11 applied at higher frequencies induces a solid-like response. The typical example usually given  
12  
13 in rheology books to illustrate this behavior is the one of a silicone ball. Such a ball left at rest  
14  
15 in a beaker for a long time will finally take the form of the beaker (viscous flow under low  
16  
17 frequency or long time sollicitation), while the same ball thrown onto a wall will bounce,  
18  
19 displaying an elastic behavior under high frequency or small time sollicitation. It is worth  
20  
21 noting that the inverse of the frequency for the moduli crossover is sometimes used as a time  
22  
23 characterizing the elasticity of the gel [29]. However, in this case, it would be delicate to  
24  
25 interpret this value since complex internal structures composed of a large number of  
26  
27 components with different lengths, flexibilities or mobilities, such as mucus simulants, are  
28  
29 most likely to display viscoelastic properties governed by the superposition of several  
30  
31 relaxation modes [2]. The low frequency crossover of moduli is not experimentally reached in  
32  
33 the case of more concentrated simulants (0.75wt% to 2wt%), for the range of tested  
34  
35 frequencies. However, in figure 5 (c),  $\tan(\delta)$  increases when the frequency decreases, so that a  
36  
37 moduli crossover would likely appear under sufficiently low frequency at a decreasing  
38  
39 frequency value, as the concentration increases, traducing an increased elasticity for more  
40  
41 concentrated mucus simulants.  
42  
43  
44  
45  
46  
47

#### 48 **Steady-state (SS) flow test**

49  
50 Steady state (SS) shear flow tests were performed on three successive samples at each  
51  
52 Actigum™ concentration. The response to the imposed stress ( $\tau$ ) is recorded in terms of  
53  
54 steady state strain rate ( $\dot{\gamma}$ ). The rheograms ( $\tau(\dot{\gamma})$  curves) drawn as the average of the three  
55  
56  
57  
58  
59  
60

1  
2  
3 measurements performed on each Actigum™ concentration displayed a similar shape for all  
4  
5 polymer concentrations. Figure 6 shows an example of such a rheogram obtained in the case  
6  
7 of a 2 wt% simulant.  
8  
9

10  
11 A yield zone with a solid-like behavior ( $\dot{\gamma} \rightarrow 0$  grey zone in figure 6) is first observed until  
12  
13 the progressive departure from a quasi vertical slope to the flow zone showing a shear-  
14  
15 thinning behavior (concave rheogram beyond the yield stress value) is reached. The yield  
16  
17 zone is the manifestation of the yielding behavior of the gel structure that has already been  
18  
19 characterized using SAOS stress amplitude sweeps tests. In SS flow mode, the transition  
20  
21 between solid and liquid-like behaviors is defined by a stress value quoted  $\tau_{0HB}$ . This value is  
22  
23 also referred in the literature as a yield stress but gives different values compared to the yield  
24  
25 stress measured in SAOS mode (see discussion part). This is why a different notation ( $\tau_{0HB}$ ) is  
26  
27 used to described this yield stress deduced from the fitting of SS flow experimental data by a  
28  
29 3 parameters Herschel-Bulkley model (equation 5) allowing to account for both the SS yield  
30  
31 stress (viscoplastic behavior) and shear-thinning behavior.  
32  
33  
34

$$\tau = \tau_{0HB} + K\dot{\gamma}^n \quad (5)$$

35  
36  
37  
38  
39  
40 where  $\tau_{0HB}$  (Pa) is the SS flow yield stress, K (Pa.s<sup>n</sup>) and n (-) are the consistency and flow  
41  
42 indexes respectively deduced from the HB modelling. It is worth noting that, as SS flow  
43  
44 curves (as well as the HB model) do not account for the time dependent flow behavior  
45  
46 (thixotropy), the observed yield stress  $\tau_{0HB}$  is not an inherent property of the material since the  
47  
48 structural strength of the gel is shear history and thus time dependent.  
49  
50

51  
52 The non Newtonian behavior observed in figure 6, is the direct consequence, in the case of  
53  
54 polymeric substances, of a shear-induced spatial structure transformation [30]. The HB model  
55  
56 parameters obtained for the different polymer concentrations are reported in table 2 and  
57  
58

1  
2  
3 account for the characterization of the steady-state flow behavior of simulants. The evolution  
4 of the different HB parameters with the Actigum™ concentration is drawn in figure 7 and  
5 clearly shows that both viscoplasticity (increase in  $\tau_{0HB}$  value) and shear-thinning behavior  
6 (increase in K, decrease in n) increase as the active polymer concentration increases. In the  
7 case of the mucus simulants studied here, an attempt has been made to propose a  
8 quantification of the different measured rheological properties. Concerning data deduced from  
9 SS flow experiments, the evolution of HB parameters with the active polymer concentration  
10 (C in wt%) can be quantified by the following empirical relationships (equations 6 to 8 ).  
11  
12  
13  
14  
15  
16  
17  
18  
19  
20

$$21 \quad \tau_{0HB} = 8.24 C^{1.34} \quad R^2 = 0.99 \quad (6)$$

$$22 \quad K = 0.315 C^{3.36} \quad R^2 = 0.974 \quad (7)$$

$$23 \quad n = 1 - 0.346 C \quad R^2 = 0.963 \quad (8)$$

24  
25  
26  
27  
28  
29  
30  
31  
32  
33  
34  
35  
36  
37  
38  
39  
40  
41  
42  
43  
44  
45  
46  
47  
48  
49  
50  
51  
52  
53  
54  
55  
56  
57  
58  
59  
60  
Equation 6 accounts for the increase in viscoplasticity, whereas equations 7 and 8 account for  
the increase in shear-thinning behavior, as the active polymer concentration increases.

### Three Interval Thixotropy Tests

3ITT tests were performed on the different simulant gels in order to investigate the thixotropic  
nature of mucus simulants independently of their SS flow behavior. Thixotropy is  
characteristic of complex internal structure systems and is linked to slow time evolutions in  
rheological properties due to either restructuring at rest or destructuring initiated by  
deformation [30]. Figure 8 represents a first 3ITT performed on a 2 wt% simulant. The second  
step imposes a shear flow under an effective shear rate of  $1.6 \text{ s}^{-1}$  corresponding to the order of  
magnitude of the shearing of a mucus layer in the tracheobronchial tree. Indeed, if the  
physiological maximum value for shear rate, can reached  $10^2\text{-}10^4 \text{ s}^{-1}$  (for example during

1  
2  
3 coughing), physiological rates in the normal lung are of the order of magnitude of  $0.1$  to  $1 \text{ s}^{-1}$ .  
4  
5 [4 ; 8 ; 14]. The three successive steps are plotted as apparent viscosity versus time.  
6

7  
8 After a shearing under  $1.6 \text{ s}^{-1}$  during step 2, one can observe in figure 8 that the thixotropic  
9 regeneration curve (step 3) allows the calculation of a thixotropic recovery time  
10 characterizing a given state of regeneration chosen here at 90% and 100% of recovery, based  
11 on the initial structure measured during step 1. The thixotropic recovery time is, in this case of  
12 2.7s for 90% and 75s for 100% of recovery.  
13  
14

15  
16  
17  
18  
19  
20 Figure 9 gives the results of a second test also performed on a 2 wt% simulant. This time, the  
21 second step corresponds to a shear flow under a larger shear rate ( $100 \text{ s}^{-1}$ ) matching the order  
22 of magnitude for the shearing of a mucus layer submitted to cough.  
23  
24

25  
26  
27 After a shearing at  $100 \text{ s}^{-1}$  during step 2, one can observe in figure 9 that the thixotropic  
28 regeneration curve (step 3) gives a 90% recovery time of 17s and a 100% recovery time of  
29 917s, which are logically higher than the recovery times needed after the shearing under  $1.6 \text{ s}^{-1}$   
30 observed in figure 8.  
31  
32  
33  
34  
35  
36  
37

## 38 **DISCUSSION**

39  
40 During stress amplitude SAOS experiments (figure 2) a  $G''$  overshoot has been observed with  
41 mucus simulants. According to Hyun et al [28-31] or Mezger [27], such an overshoot is  
42 generally obtained in the case of cross-linked polymers or gel-like internal structures  
43 (existence of a 3D network). The overshoot is directly linked to the progressive collapse of  
44 the 3D network. During the initiation of flow, at first the friction increases due to spatial  
45 rearrangements of some free elements (for example relative motion of end pieces of chains).  
46 These irreversible motions induce an increase in dissipated energy ( $G''$  increases). Then the  
47 breakdown of the internal superstructure occurs (at the  $\tau_{\text{peak}}$  value) and the dissipated energy  
48  
49  
50  
51  
52  
53  
54  
55  
56  
57

1  
2  
3 starts decreasing as the fluid actually flows. In the case of mucus simulants used in this work,  
4  
5 the overshoot behavior shows a strong dependency on the Actigum™ concentration. On the  
6  
7 one hand, the  $\tau_{\text{peak}}$  value increases as the simulant concentration increases (figure 3(a) and eq.  
8  
9 3 for quantification). This is not surprising since more concentrated simulants have a stronger  
10  
11 internal network that will need a higher energy input to collapse. On the other hand, the peak  
12  
13 height is also increasing with the Actigum™ concentration (figure 2(b)). The overshoot  
14  
15 amplitude is directly linked to the amount of friction occurring during the initiation of flow due  
16  
17 to spatial rearrangements of free elements. A more concentrated sample is thus expected to  
18  
19 dissipate more friction energy as a result of its higher network density (more cross-linking and  
20  
21 chains entanglements). A  $G''$  overshoot during stress amplitude sweeps was rarely mentioned  
22  
23 in the literature on the rheological characterization of mucus. In the work of Bastholm [9], a  
24  
25  $G''$  overshoot seems to occur with some of the tested cervical mucus samples, without any  
26  
27 comment concerning this phenomenon. Celli *et al.* [5], performing a SAOS stress amplitude  
28  
29 sweep on a sane gastric mucus sample (compared to a *Helicobacter pylori* contaminated one),  
30  
31 also observed a "weak strain overshoot" on  $G''$  and referred to the work of Huyn *et al.* [28] for  
32  
33 interpretation. Concerning now the internal network volumetric energy of cohesion  $E_c$  values,  
34  
35 we can refer to works by Mori *et al.* [32] or Niraula *et al.* [26] for comparison purposes. Based  
36  
37 on SAOS characterizations on respectively biological suspensions or stabilized oil in water  
38  
39 (O/W) emulsions both exhibiting a 3D cohesive network, they calculated the volumetric  
40  
41 cohesive energy of the material internal network to account for the degree of interaction and  
42  
43 thus of flocculation between droplets in the case of stabilized O/W emulsions [26] and  
44  
45 between bioflocs in the case of activated sludge suspensions [32]. The mucus simulants  
46  
47 studied here are not flocculated suspensions nor liquid-liquid emulsions but aqueous  
48  
49 dispersions of macromolecules. However since a 3D network exists both due to entanglement  
50  
51 and cross-linking of the macromolecules the concept of volumetric cohesive energy can be  
52  
53  
54  
55  
56  
57  
58  
59  
60

1  
2  
3 useful to quantitatively account for the degree of interaction of the subsequent network. One  
4  
5 can observe that the order of magnitude of  $E_c$  for the Actigum<sup>TM</sup> based mucus simulants (0.02  
6  
7 to  $0.36 \text{ J.m}^{-3}$ ) is intermediate between  $E_c$  values calculated for biological activated sludge  
8  
9 suspensions [32] ( $0.2$  to  $1.2 \text{ J.m}^{-3}$ ) and  $E_c$  values of stabilized O/W emulsions ( $0.24 \cdot 10^{-3}$  to  
10  
11  $2.95 \cdot 10^{-3} \text{ J.m}^{-3}$ ). It is also worth noting that  $E_c$  values showed important dependence upon the  
12  
13 network macromolecular or suspended bioflocs concentration (power law (eq. 4) in this work,  
14  
15 exponential law in [32]). The influence of the polymer concentration on stress amplitude  
16  
17 SAOS measurements displayed in figure 3 for synthetic mucus, has been discussed in some  
18  
19 previous works. As an example, Riley et al. [7] showed that an increase in polymer (Carbopol  
20  
21 934P) concentration induced an increase in both  $G'$  and  $G''$  measured in the LVE range at a  
22  
23 constant (5 Hz) frequency. Shah et al. [19] also observed working with mucus simulants that  
24  
25 both  $G'$  and  $G''$  (either measured at 1 or 100 rad/s) increased with the coagulant concentration  
26  
27 (0.5, 1.5 and 3%). Finally, Hamel & Fiegl [10] measured an identical increase with cross-  
28  
29 linked polymer concentration of  $G'$  and  $G''$  moduli, performing on synthetic mucus strain  
30  
31 sweeps at a constant frequency. Nevertheless, in all of these previous studies, the observed  
32  
33 variations were not quantified. An interesting point that can however be pointed out is the fact  
34  
35 that the achieved order of magnitude of  $G'$  and  $G''$  (in the LVE range) with the mucus  
36  
37 simulants tested in this work correspond to those usually observed with sane or pathologic  
38  
39 native respiratory mucus. For instance, CF mucus can reach various viscoelasticity levels as a  
40  
41 function of many factors. In the work of Dawson et al. [18] CF mucus displays viscoelastic  
42  
43 properties, in terms of moduli plateau values, close to those displayed by the 2wt%  
44  
45 Actigum<sup>TM</sup> gel while in the research of Yuan et al. [11], the measured behavior is close to the  
46  
47 one measured with the 0.75wt% gel. Concerning sane mucus, moduli plateau values close to  
48  
49 those recorded with the 0.5wt% solution have been observed [11]. Concerning the effect of  
50  
51 temperature on the LVE range limit, identical results to those shown in figure 4 have been  
52  
53  
54  
55  
56  
57  
58  
59  
60

1  
2  
3 described for mucus gels with similar composition, in the same temperature range (20, 32 or  
4  
5 36°C) [33]. A very limited influence of temperature on simulants rheological properties  
6  
7 measured both via stress amplitude sweeps and flow curves was recorded by the authors.  
8  
9 Taylor et al. [6], who studied the rheological characterization of mucin - alginate gels, also  
10  
11 reported no significant differences between the gels behaviors (frequency sweep tests) over a  
12  
13 10 to 60°C temperature range. The rheological properties of such aqueous polyoside solutions  
14  
15 are known to be related to the conformation taken by the macromolecules (Viscogum<sup>TM</sup> &  
16  
17 Actigum<sup>TM</sup>). Mucus simulants studied here are composed of a constant amount of  
18  
19 Viscogum<sup>TM</sup> (galactomannan chains that are cross-linked in the presence of sodium  
20  
21 tetraborate) and various proportions of Actigum<sup>TM</sup> (extracellular polyoside) that can adopt  
22  
23 either a rigid helicoidal conformation or a random entangled conformation, as a function  
24  
25 notably of temperature [29]. From the measurements displayed in figure 4, it can be  
26  
27 concluded that Actigum<sup>TM</sup> molecules are likely to present the rigid helicoidal conformation in  
28  
29 simulants tested here, leading to the observed gel-like behavior ( $G' > G''$ ) and also that this  
30  
31 conformation remains when the temperature is raised to values such as 37°C.  
32  
33  
34  
35  
36

37 During frequency SAOS sweeps, we obtained results (figure 5) that are, for 0.75 to 2wt%  
38  
39 gels, qualitatively comparable to those observed by Coussot et Grossiord [29] on a 0.5wt%  
40  
41 xanthan gum aqueous solution at 25°C. Xanthan gum is an extracellular polyoside close to  
42  
43 Actigum<sup>TM</sup> in terms of macromolecular composition and structure (glucose chain branched  
44  
45 every 2 units by other oside functions forming a 3D rigid double helix structure), exhibiting  
46  
47 very similar rheological properties. The gel-like behavior of aqueous xanthan solutions over  
48  
49 the whole frequency range is known to be linked to the helicoidal rigid conformation adopted  
50  
51 by polyoside molecules under moderate temperatures or high ionic strength, impairing their  
52  
53 ability to move under small sollicitations. In the case of Actigum<sup>TM</sup> aqueous solutions,  
54  
55  
56  
57  
58  
59  
60

1  
2  
3 Actigum<sup>TM</sup> macromolecules are also known to adopt a rigid triple helix conformation (except  
4  
5 under high temperatures or low ionic strength) that is responsible for the gel-like response  
6  
7 measured over the entire range of tested frequencies in the case of 0.75wt% to 2wt%  
8  
9 Actigum<sup>TM</sup> gels. Kocevar-Nared et al. [23] also made observations qualitatively comparable  
10  
11 to figure 5 in the case of rehydrated dried crude porcine gastric mucus. Varying the mucin  
12  
13 concentration of rehydrated mucus, they observed that more concentrated samples displayed  
14  
15 no moduli crossover (in the 0.1 - 100 Hz explored range) but a power law slight frequency  
16  
17 dependence for both moduli whereas, more diluted sample displayed a stronger frequency  
18  
19 dependence for both moduli whereas, more diluted sample displayed a stronger frequency  
20  
21 dependence with a crossover point moving towards lower frequencies as the mucin  
22  
23 concentration is increased and as the structure changes to gel-like. In the case of the 0.5wt%  
24  
25 gel studied here, the stronger dependence to the frequency can be linked to the increase in  
26  
27 relative importance of Viscogum<sup>TM</sup> (flexible entangled network) compared to Actigum<sup>TM</sup>  
28  
29 (rigid network) in comparison to gels with higher Actigum<sup>TM</sup> concentrations.  
30

31  
32 During SS flow measurements, the concentration dependent yield stress and shear-thinning  
33  
34 nature of mucus simulants has been observed (figure 6) and quantify (equations 6 to 8).  
35  
36 Identical observations have already been reported but only qualitatively in the case of mucus  
37  
38 simulants and native mucus based on measurements of their rheological flow behavior. The  
39  
40 increase in viscoplasticity (yield stress) with the active polymer concentration has already  
41  
42 been observed in the SAOS stress amplitude tests section of the paper. Yield stresses  
43  
44 measured in flow mode  $\tau_{0HB}$  show higher values than yield stresses measured in SAOS  $\tau_y$ .  
45  
46 This is not surprising since  $\tau_y$  corresponds to the end of the LVE range characterized by early  
47  
48 motions of small elements of the complex internal polymeric structure (at the microscopic  
49  
50 level), while  $\tau_{0HB}$  corresponds to the proper beginning of flow measured at a macroscopic  
51  
52 scale (existence of a finite shear rate in the measuring gap). It is also worth noting that both  $\tau_y$   
53  
54  
55  
56  
57  
58  
59  
60

1  
2  
3 and  $\tau_{0HB}$  values are dependent on the calculation method (chosen % of deviation from the  
4  
5  
6 plateau for  $\tau_y$  and chosen limit value for  $\dot{\gamma} \rightarrow 0$  in the case of  $\tau_{0HB}$ ). As a consequence, both  
7  
8  
9 values should only be considered as order of magnitudes or for comparison purposes of data  
10  
11  
12 obtained using the same calculation method. As far as the evolution of yield stresses with the  
13  
14  
15 active concentration is concerned, Malkin et al. [34] reported the case of cysteine / Ag based  
16  
17  
18 colloidal gels for which the yield stress deduced from flow measurements decreases as the  
19  
20  
21 dilution factor of the initial gel increases, showing the decrease in strength of the rigid  
22  
23  
24 structure as the colloidal concentration decreases. If we now focus on the observed shear-  
25  
26  
27 thinning properties of mucus simulants, Puchelle et al. [13] also described the shear-thinning  
28  
29  
30 nature of native and lyophilized pathological bronchial mucus but also of simulants composed  
31  
32  
33 of polyisobutylene solutions (3 and 6% in decalin). Measuring the SS flow curve of these  
34  
35  
36 gels, they obtained shear-thinning indexes (Ostwald de Waele or power law) matching the  
37  
38  
39 range observed in table 2 with our mucus simulants and varying from 0.44 to 0.64. Banerjee  
40  
41  
42 et al. [14] also used a power law to describe the apparent viscosity of shear-thinning mucus  
43  
44  
45 simulants (tragacanth gum) mixed with different surfactants to evaluate their ability to reduce  
46  
47  
48 viscosity. They obtained viscosity reduction ratios varying from 1.5 to 7.2 depending on the  
49  
50  
51 type of surfactant under physiological shear rates (0.1 to 1 s<sup>-1</sup> in the tracheobronchial tree).  
52  
53  
54 The shear-thinning behavior of mammalian lung mucus is also cited by Vasquez et al. [16]  
55  
56  
57 but not quantified. It is also the case of Boegh et al. [21] who tried to propose a bio-similar  
58  
59  
60 mucus composition displaying rheological properties (notably in terms of shear-thinning)  
close to the composition of a mucus isolated from cultured cells. Finally, Tomaiuolo et al.  
[24] also described the shear-thinning nature of different native CF mucus samples without  
proposing any quantification of this property. More generally, the increase in shear-thinning  
behavior with the polymer concentration, is classical for aqueous polymer solutions. It

1  
2  
3 corresponds to an increase in shear-thinning capacity for solutions with a higher  
4 macromolecular content due to a concentration enhanced reduction of the flow resistance  
5 following the alignment and orientation of polymeric chains in the flow direction as the shear  
6 rate increases [17 ; 23 ; 34]. Shah et al. [19] compared viscosity curves of respiratory mucus  
7 simulants (0.5 to 3% in polyox resin coagulant). However, they only discussed their results in  
8 terms of viscosity increase with the coagulant concentration and did not account for the shear-  
9 thinning nature of the studied fluids, nor for its evolution with the polymer concentration.  
10  
11  
12  
13  
14  
15  
16  
17  
18  
19  
20  
21  
22  
23  
24  
25  
26  
27  
28  
29  
30  
31  
32  
33  
34  
35  
36  
37  
38  
39  
40  
41  
42  
43  
44  
45  
46  
47  
48  
49  
50  
51  
52  
53  
54  
55  
56  
57  
58  
59  
60

Finally, 3ITTs performed on a 2wt% simulant gel (figures 8 & 9) allow measuring thixotropic recovery times. If the thixotropic nature of native or synthetic mucus has been reported in some of the previous works devoted to mucus rheological characterization [1 ; 22 ; 23 ; 24], it has often not been quantified. Nielsen et al. [22] but also Tomaiuolo et al. [24], described qualitatively the thixotropic nature of native samples observing an hysteresis loop between viscosity curves successively measured at increasing or decreasing shear rates. Kocevar et al. [23] recorded with porcine gastric mucins solutions at concentrations varying from 10 to 60% the apparent viscosity versus time under a constant shear rate of  $50 \text{ s}^{-1}$ . They concluded depending on the appearance of a viscosity decrease versus time, that gels above 30% are thixotropic while lower concentrated one showed no thixotropy. Zahm et al. [1] performed identical measurements on mucus simulants and calculated a thixotropic index based on the stress evolution with time under a  $1.6 \text{ s}^{-1}$  shear rate. The thixotropic index was calculated by the ratio of the initial stress value to the plateau stress value and gave values between 1 (no thixotropy) and 1.8 depending on the samples. However, based on our experiments, since two

1  
2  
3 different rheometers have been tested here, it seems that the initial stress overshoot height  
4  
5 may be dependent on the response time of the rheometer. Indeed, the more precise DHR-2  
6  
7 (TA Instruments) rheometer gave on the same sample a higher stress overshoot than the  
8  
9 AR500 rheometer (TA Instruments). As a consequence, thixotropic indexes should not be  
10  
11 compared when measured with different apparatus. To the authors' knowledge, 3ITTs results  
12  
13 on mucus or mucus simulants have never been published. For comparison purposes however,  
14  
15 we can refer to the recent work of Toker et al. [30] describing the results of 3ITTs performed  
16  
17 on a mayonnaise or to the work of Mezger [35] in which identical 3ITTs are compared for  
18  
19 two different paints. For a  $100 \text{ s}^{-1}$  step 2 in both studies, Toker et al. [30] measured a 100%  
20  
21 recovery time varying of 56 to 432 s for a mayonnaise depending on the temperature, while  
22  
23 Mezger [35] measured a 100% recovery time of 60 s or 300 s for the two paint samples  
24  
25 (temperature not given). These results indicate that mucus simulants tested here show a  
26  
27 slower thixotropic recovery compared to paints or mayonnaises (often used as "model"  
28  
29 thixotropic fluids) investigated in these previous works. To conclude with thixotropy, it is  
30  
31 obvious that the thixotropic nature of mucus simulants can give rise to much more studies. In  
32  
33 particular, it would be interesting to perform an important set of 3ITTs with step 2 covering  
34  
35 intermediate shear rate values between  $1 \text{ s}^{-1}$  and  $100 \text{ s}^{-1}$ . Modelling these experiments, a time  
36  
37 dependent rheological model for mucus simulants at each active polymer concentration, could  
38  
39 then be deduced. Such a time dependent model could be useful to account for the whole  
40  
41 rheological complexities of these gels and could for instance allow to simulate their behavior  
42  
43 in a model trachea, when submitted to various air pressure signals, such as signals imposed by  
44  
45 clearance helping devices. This will be the purpose of a future work.  
46  
47  
48  
49  
50

51  
52 In conclusion, in this work, a complete and quantified rheological characterization has been  
53  
54 performed on mucus simulants at different active polymer concentrations (0.5wt% to 2wt% in  
55  
56  
57

1  
2  
3 Actigum<sup>TM</sup>). Stress amplitude SAOS sweeps first allowed determining the LVE range of these  
4  
5 gels at 20°C. To account for the end of the LVE range and the subsequent transition towards  
6  
7 flow, different transition stresses (namely, yield  $\tau_y$ , flow  $\tau_f$  and peak  $\tau_{peak}$  stresses) were  
8  
9 described. The increase of these transition stresses with Actigum<sup>TM</sup> concentration showed a  
10  
11 power law dependence (eq. 2 & 3). Based on the yield stress value and the corresponding  
12  
13 critical deformation, a cohesive volumetric energy ( $J.m^{-3}$ ) that also followed an active  
14  
15 concentration increasing power law (eq. 4) was calculated. Elastic and viscous moduli plateau  
16  
17 values indicated, for all gel concentrations, stability ( $G' > G''$ ), as well as a linear increase  
18  
19 with the Actigum<sup>TM</sup> concentration. The temperature dependence of the LVE range was not  
20  
21 significant in the range between 20 and 37 °C. Frequency SAOS sweeps displayed, only in  
22  
23 the case of the lowest active polymer concentration, a low frequency moduli cross-over,  
24  
25 showing the liquid-like behavior of this gel under very slow sollicitation and its solid-like  
26  
27 behavior under relatively rapid sollicitation. More concentrated gels displayed a solid-like  
28  
29 behavior over the whole range of tested frequencies. However, based on the  $\tan(\delta)$  evolution  
30  
31 one can anticipate a moduli cross-over under lower frequencies as the Actigum<sup>TM</sup>  
32  
33 concentration increases. In flow mode, to separate viscoplasticity and shear-thinning from  
34  
35 thixotropy, steady state flow curves were recorded and the HB model was used to quantify  
36  
37 simulants SS viscoplasticity (via a yield stress measured in flow mode  $\tau_{0HB}$ ) and shear-  
38  
39 thinning property (via the consistency (K) and flow indexes (n)). The evolutions of these  
40  
41 parameters with the Actigum<sup>TM</sup> concentration displayed a power law increase for  $\tau_{0HB}$  and K  
42  
43 (eq. 6 & 7) and a linear decrease for n (eq. 8) indicating an enhanced viscoplasticity and  
44  
45 shear-thinning ability for more concentrated gels. Finally the thixotropy of a 2wt% gel was  
46  
47 tested performing two 3ITTs, submitting the sample to shear rates representative of normal  
48  
49 shearing in the lungs ( $1.6 s^{-1}$ ) or special events such as cough ( $100 s^{-1}$ ). To quantify thixotropy  
50  
51 it was proposed to evaluate a recovery time based on either 90% or 100% of recovery of the  
52  
53  
54  
55  
56  
57  
58  
59  
60

1  
2  
3 initial structure. Concerning this latter property, further investigations are necessary to fully  
4  
5 characterize the thixotropic nature of mucus simulants, in particular to propose a time  
6  
7 dependent rheological. This is clearly an interesting prospect for future works.  
8  
9

## 10 11 **ACKNOWLEDGMENTS**

12  
13  
14 The authors are indebted to the PhysioAssist Co. and the Association Nationale de la  
15  
16 Recherche et de la Technologie for the CIFRE grant 2014-1287 (O. Lafforgue PhD thesis)  
17  
18 and to the Laserson Co. for kindly providing the Actigum<sup>TM</sup> and Viscogum<sup>TM</sup> polymers. S.  
19  
20 Poncet acknowledges also the Canada Foundation for Innovation (John R. Evans Leaders  
21  
22 Fund n°34582) and the Natural Sciences and Engineering Research Council of Canada  
23  
24 through the Discovery Grant (RGPIN-2015-06512) for their financial support.  
25  
26  
27

## 28 29 **REFERENCES**

- 30  
31 [1] Zahm J.M., King M., Duvivier C., Pierrot D., Girod S. and Puchelle E. Role of simulated  
32  
33 repetitive coughing in mucus clearance. *European Respiratory Journal*, 1991, 4(3), p.311–315.
- 34  
35 [2] Vasquez P. A. and Forest M. G.. “Complex fluids and soft structures in the human body”.  
36  
37 *Complex Fluids in Biological Systems*, Springer Science, S.E. Spagnolie (ed.), New-York,  
38  
39 2015, pp. 53-110.
- 40  
41 [3] Thornton D.J. and Sheehan J.K. From mucins to mucus: toward a more coherent  
42  
43 understanding of this essential barrier. *Proceedings of the American Thoracic Society*, 2004,  
44  
45 1(1), p.54-61.
- 46  
47 [4] Lai S. K., Wang Y-Y., Wirtz D., and Hanes J. Micro- and macrorheology of mucus.  
48  
49 *Advanced Drug Delivery Reviews* 61, 2009, pp. 86-100.
- 50  
51 [5] Celli J. P., Turner B. S., Afdhal N. H., Keates S., Ghiran I., Kelly C. P., Ewoldt R. H.,  
52  
53 McKinley G. H., So P., Erramilli S., Bansil R., and Austin R. H. Helicobacter pylori moves  
54  
55 through mucus by reducing mucin viscoelasticity. *Proceedings of the National Academy of*  
56  
57 *Sciences of the United States of America*, 2009, 106(34):14321.
- 58  
59 [6] Taylor C., Pearson J.P., Draget K.I., Dettmar P.W., Smidsrod O., Rheological  
60  
characterisation of mixed gels of mucin and alginate, *Carbohydrate polymers*, 2005, 59, 189-  
195.
- [7] Riley R.G., Smart J.D., Tsibouklis J., Dettmar P.W., Hampson F., Alf Davis J., Kelly G.,  
Wilber W.R., An investigation of mucus/polymer synergism using synthesised and  
characterised poly(acrylic acid)s, *International Journal of Pharmaceutics*, 2001, 217, 87-100.

- 1  
2  
3 [8] Aubuchon S.R. and Rubin B.K. Application of viscoelastic transformations to rheological  
4 analysis of human biological fluids. 1998, New Castle DE: TA Instruments.  
5  
6 [9] Bastholm S. K., Becher N., Stubbe P. R., Chronakis I. S., and Uldbjerg N. The viscoelastic  
7 properties of the cervical mucus plug. *Acta Obstetricia et Gynecologica Scandinavica*, 2014,  
8 93(2):201 – 208.  
9  
10 [10] Hamed R. and Fiegel J. Synthetic tracheal mucus with native rheological and surface  
11 tension properties. *Journal of biomedical materials research*. 2001, Part A, 102(6):1788 –  
12 1798.  
13  
14 [11] Yuan S., Hollinger M., Lachowicz-Scroggins M. E, Kerr S. C., Dunican E. M., Daniel B.  
15 M., Ghosh S., Serpel C Erzurum, Belinda Willard, Stanley L Hazen, Xiaozhu Huang, Stephen  
16 D Carrington, Oscarson S., and Fahy J.V. Oxidation increases mucin polymer cross-links to  
17 stiffen airway mucus gels. *Science Translational Medicine*, 2015, 7(276):276ra27.  
18  
19 [12] Taylor Nordgard C. and Draget K. I. Oligosaccharides as modulators of rheology in  
20 complex mucous systems *Biomacromolecules*, 2011, 12(8):3084 – 3090.  
21  
22 [13] Puchelle E., Zahm J.M., Duvivier C., Didelon J., Jacquot J., and Quemada. D.  
23 Elastothixotropic properties of bronchial mucus and polymer analogs. i. experimental results.  
24 *Biorheology*, 1985, volume 22, pages 415 - 423.  
25  
26 [14] Banerjee R., Bellare J.R., Puniyani R.R., Effect of phospholipid mixtures and surfactant  
27 formulations on rheology of polymeric gels, simulating mucus, at shear rates experienced in  
28 the tracheobronchial tree, *Biochemical Engineering Journal*, 2001, 7, 195-200.  
29  
30 [15] Lee C.H., Wang Y., Shin S-C., Chien Y.W., Effects of chelating agents on the  
31 rheological property of cervical mucus, *Contraception*, 2002, 65435-440.  
32  
33 [16] Vasquez E. S., Bowser J., Swiderski C., Walters K. B., and Kundu S. Rheological  
34 characterization of mammalian lung mucus. *RSC Advances*, 2014, 4(66):34780.  
35  
36 [17] Bhat P. G., Flanagan D. R., and Donovan M. D. Drug diffusion through cystic fibrotic  
37 mucus: steady-state permeation, rheologic properties, and glycoprotein morphology. *Journal*  
38 *Of Pharmaceutical Sciences*, 1996, 85(6):624 – 630.  
39  
40 [18] Dawson M., Wirtz D., and Hanes J. Enhanced viscoelasticity of human cystic fibrotic  
41 sputum correlates with increasing microheterogeneity in particle transport. *The Journal Of*  
42 *Biological Chemistry*, 2003, 278(50):50393 – 50401.  
43  
44 [19] Shah S., Fung K., Brim S. and Rubin B.K., An in vitro evaluation of the effectiveness of  
45 endotracheal suction catheters, *Chest*, 2005, 128 (5), p.3699-3704.  
46  
47 [20] Celli J. P., Turner B. S, Afdhal N. H., Ewoldt R. H, Mckinley G. H., Rama Bansil, and  
48 Erramilli S. Rheology of gastric mucin exhibits a ph-dependent sol-gel transition,  
49 *Biomacromolecules*, 2001, 8(5):1580 – 1586.  
50  
51 [21] Boegh M., Baldursdóttir S. G, Nielsen M. H., Müllertz A., and Nielsen H. M.  
52 developement and rheological profiling of biosimilar mucus. *Annual transaction of th enordic*  
53 *rheology society*, 2013, vol 11, 233-240.  
54  
55  
56  
57  
58  
59  
60

- 1  
2  
3 [22] Nielsen H., Hvidt S., Sheils C.A. and Janmey P.A. Elastic contributions dominate the  
4 viscoelastic properties of sputum from cystic fibrosis patients. *Biophysical Chemistry*, 2004,  
5 112, p.193-200.  
6  
7 [23] Kocevar-Nared J., Kristl J., Smid-Korbar J., Comparative rheological investigation of  
8 crude gastric mucin and natural gastric mucus, *Biomaterials*, 1997, 18, 677-681.  
9  
10 [24] Tomaiuolo G., Rusciano G., Caserta S., Carciati A., Carnovale V., Abete P., Sasso A.,  
11 and Guido S. A new method to improve the clinical evaluation of cystic fibrosis patients by  
12 mucus viscoelastic properties. *Plos One*, 2014, 9(1):e82297.  
13  
14 [25] Coussot P and Ancey C. Rheophysical classification of concentrated suspensions and  
15 granular pastes. *The American Physical Society* 1999;59:4445-57.  
16  
17 [26] Niraula B., King T.C., Misran M., Evaluation of rheological property of dodecyl  
18 maltoside, sucrose dodecanoate, Brij 35p and SDS stabilized O/W emulsion: effect of head  
19 group structure on rheology property and emulsion stability, *colloides and Surfaces A.*, 2004,  
20 251, 59-74.  
21  
22 [27] Mezger T.G.. *The Rheology Handbook: For Users of Rotational and Oscillatory*  
23 *Rheometers.* European Coatings. Vincentz Network, 2014.  
24  
25 [28] Hyun K., Kim S.H., Ahn K.H., Lee S.J., “Large amplitude oscillatory shear as a way to  
26 classify the complex fluids”, *J. Non-Newtonian Fluid Mech.*, 2002, **107**, pp. 51-65.  
27  
28 [29] Coussot P., and Grossiord J-L., *Comprendre la rhéologie de la circulation du sang à la*  
29 *prise du béton*, EDP sciences, 2001.  
30  
31 [30] Toker O.S., Karusa S., Yilmaz M.T., Karaman S., 3ITT in food applications: a novel  
32 technique to determine structural regeneration of mayonnaise under different shear conditions,  
33 *Food research International*, 2015, 70, 125-133.  
34  
35 [31] Hyun K., Wilhelm M., Klein C. O., Cho K. S., Nam J. G., Ahn K. H., Lee S. J., Ewoldt  
36 R. H., and McKinley G. H., A review of nonlinear oscillatory shear tests: Analysis and  
37 application of large amplitude oscillatory shear (laos). *Progress in Polymer Science*, 2011, **36**,  
38 pp. 1697-1753.  
39  
40 [32] Mori M., Seyssiecq I., Roche N., Rheological measurements of sewage sludge for various  
41 solids concentrations and geometry, *Process Biochemistry*, 2006, 41, 1656-1662.  
42  
43 [33] Seyssiecq Guarente I., Poncet S. *Etude sur la caractérisation rhéologique du mucus*  
44 *bronchique. Premiers résultats sur fluides modèles. rapport confidentiel*, 2012.  
45  
46 [34]. Malkin A.Ya., Non-Newtonian viscosity in steady state shear flows, *J. Non-Newtonian*  
47 *Fluid Mechanics*, 2013, 192, 48-65.  
48  
49 [35] Mezger T.G., *applied rheology Anton Paar GmbH*, 2015.  
50  
51  
52  
53  
54  
55  
56  
57  
58  
59  
60

1  
2  
3  
4 **FIGURE LEGENDS**  
5

6  
7 **Figure 1:** SAOS sweeps for a 1.5wt% sample. (a) Stress sweep ( $\frac{1}{2\pi}$  Hz) (b) Frequency  
8 sweep (1Pa).  
9

10  
11  
12  
13 **Figure 2 :** Evolution of G' (a), G'' (b), tan( $\delta$ ) (c) vs stress amplitude for different  
14 Actigum<sup>TM</sup> concentrations  
15

16  
17  
18 **Figure 3:** (a) Limit stresses for LVE range & E<sub>c</sub> (b) G' & G'' plateau values vs. Actigum<sup>TM</sup>  
19 concentration  
20

21  
22  
23 **Figure 4:** Evolution of G' and G'' vs. stress amplitude at either 20°C or 37°C for a 0.75wt%  
24 gel at  $\frac{1}{2\pi}$  Hz  
25  
26

27  
28  
29  
30 **Figure 5:** Evolution of G' (a), G'' (b) and tan( $\delta$ ) (c) vs frequency for different  
31 Actigum<sup>TM</sup> concentrations  
32

33  
34  
35 **Figure 6:** SS rheogram of a 2wt% simulant  
36

37  
38  
39 **Figure 7:** HB model parameters vs. Actigum<sup>TM</sup> concentration  
40

41  
42 **Figure 8:** 3ITT step 1 at 0.029 s<sup>-1</sup>, step 2 at 1.6s<sup>-1</sup>, step 3 at 0.029 s<sup>-1</sup>  
43

44  
45 **Figure 9:** 3ITT step 1 at 0.029 s<sup>-1</sup>, step 2 at 100 s<sup>-1</sup>, step 3 at 0.029 s<sup>-1</sup>  
46  
47  
48  
49  
50  
51  
52  
53  
54  
55  
56  
57  
58  
59  
60

1  
2  
3  
4  
5  
6  
7  
8  
9  
10  
11  
12  
13  
14  
15  
16  
17  
18  
19  
20  
21  
22  
23  
24  
25  
26  
27  
28  
29  
30  
31  
32  
33  
34  
35  
36  
37  
38  
39  
40  
41  
42  
43  
44  
45  
46  
47  
48  
49  
50  
51  
52  
53  
54  
55  
56  
57  
58  
59  
60

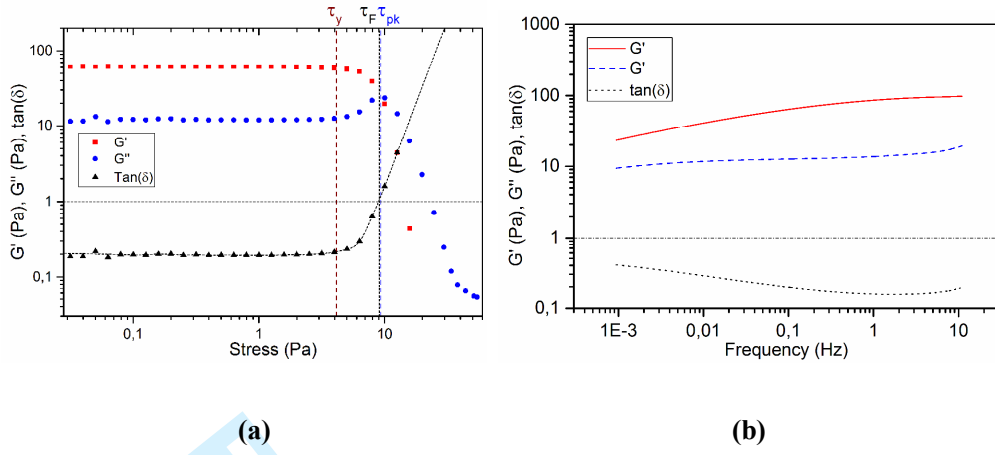


Figure 1.

For Peer Review

1  
2  
3  
4  
5  
6  
7  
8  
9  
10  
11  
12  
13  
14  
15  
16  
17  
18  
19  
20  
21  
22  
23  
24  
25  
26  
27  
28  
29  
30  
31  
32  
33  
34  
35  
36  
37  
38  
39  
40  
41  
42  
43  
44  
45  
46  
47  
48  
49  
50  
51  
52  
53  
54  
55  
56  
57  
58  
59  
60

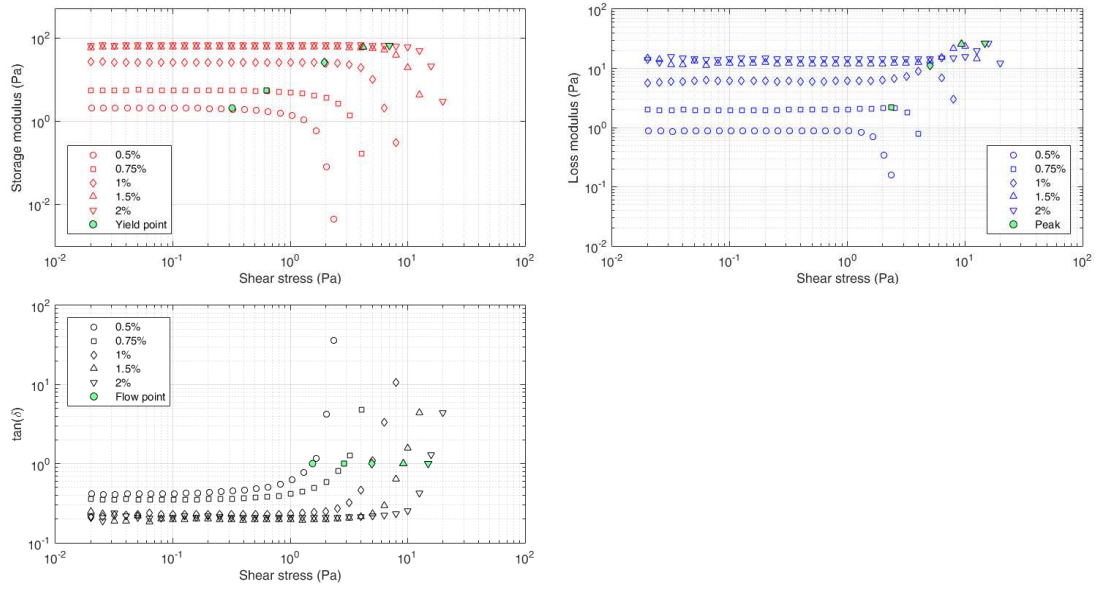


Figure 2

Peer Review

1  
2  
3  
4  
5  
6  
7  
8  
9  
10  
11  
12  
13  
14  
15  
16  
17  
18  
19  
20  
21  
22  
23  
24  
25  
26  
27  
28  
29  
30  
31  
32  
33  
34  
35  
36  
37  
38  
39  
40  
41  
42  
43  
44  
45  
46  
47  
48  
49  
50  
51  
52  
53  
54  
55  
56  
57  
58  
59  
60

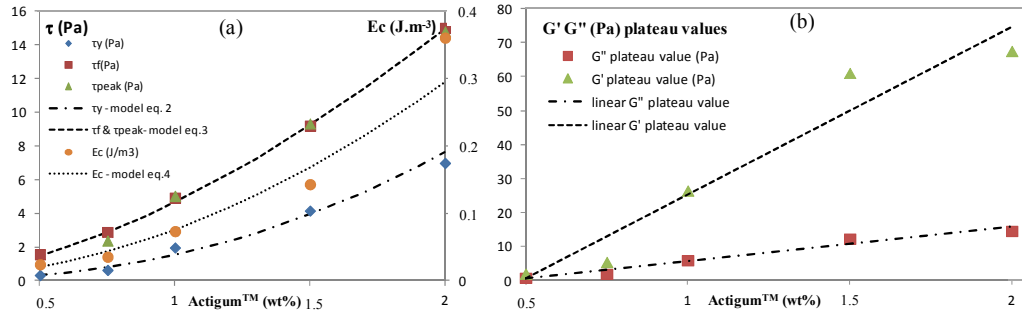


Figure 3

For Peer Review

1  
2  
3  
4  
5  
6  
7  
8  
9  
10  
11  
12  
13  
14  
15  
16  
17  
18  
19  
20  
21  
22  
23  
24  
25  
26  
27  
28  
29  
30  
31  
32  
33  
34  
35  
36  
37  
38  
39  
40  
41  
42  
43  
44  
45  
46  
47  
48  
49  
50  
51  
52  
53  
54  
55  
56  
57  
58  
59  
60

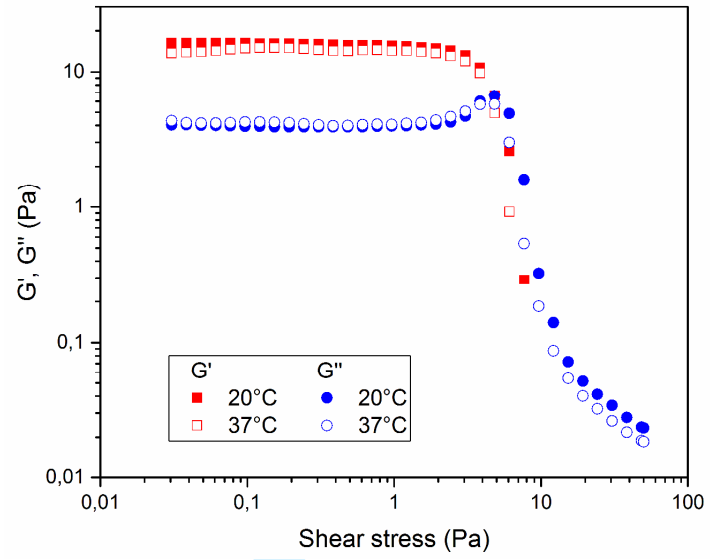


Figure 4

Peer Review

1  
2  
3  
4  
5  
6  
7  
8  
9  
10  
11  
12  
13  
14  
15  
16  
17  
18  
19  
20  
21  
22  
23  
24  
25  
26  
27  
28  
29  
30  
31  
32  
33  
34  
35  
36  
37  
38  
39  
40  
41  
42  
43  
44  
45  
46  
47  
48  
49  
50  
51  
52  
53  
54  
55  
56  
57  
58  
59  
60

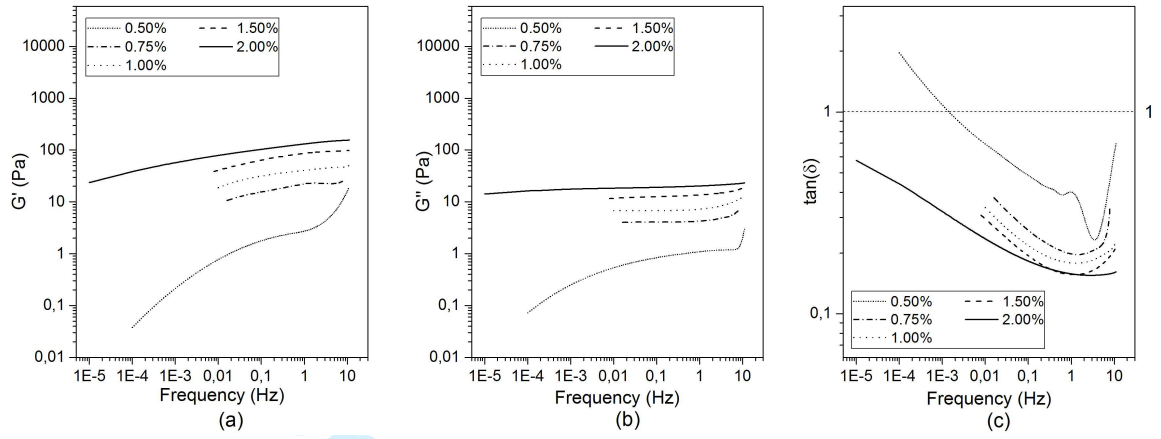


Figure 5

Peer Review

1  
2  
3  
4  
5  
6  
7  
8  
9  
10  
11  
12  
13  
14  
15  
16  
17  
18  
19  
20  
21  
22  
23  
24  
25  
26  
27  
28  
29  
30  
31  
32  
33  
34  
35  
36  
37  
38  
39  
40  
41  
42  
43  
44  
45  
46  
47  
48  
49  
50  
51  
52  
53  
54  
55  
56  
57  
58  
59  
60

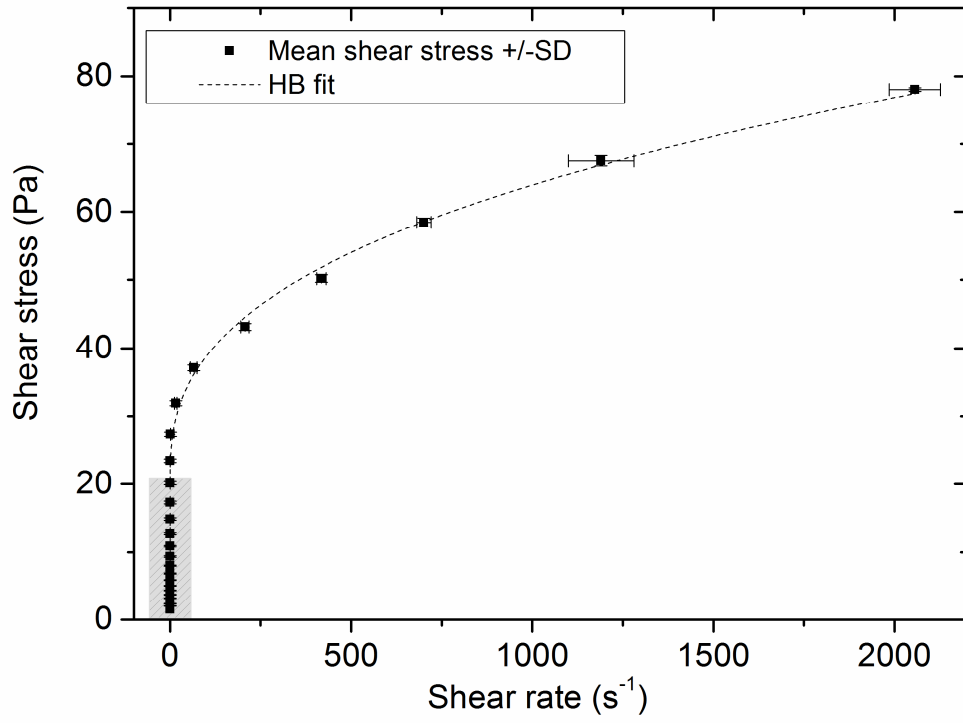


Figure 6: SS rheogram of a 2wt% simulant

Review

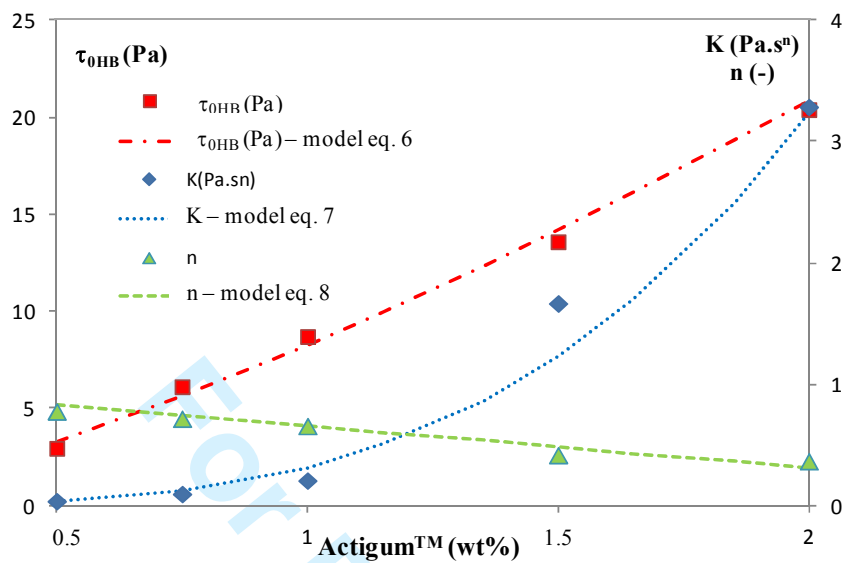


Figure 7

1  
2  
3  
4  
5  
6  
7  
8  
9  
10  
11  
12  
13  
14  
15  
16  
17  
18  
19  
20  
21  
22  
23  
24  
25  
26  
27  
28  
29  
30  
31  
32  
33  
34  
35  
36  
37  
38  
39  
40  
41  
42  
43  
44  
45  
46  
47  
48  
49  
50  
51  
52  
53  
54  
55  
56  
57  
58  
59  
60

1  
2  
3  
4  
5  
6  
7  
8  
9  
10  
11  
12  
13  
14  
15  
16  
17  
18  
19  
20  
21  
22  
23  
24  
25  
26  
27  
28  
29  
30  
31  
32  
33  
34  
35  
36  
37  
38  
39  
40  
41  
42  
43  
44  
45  
46  
47  
48  
49  
50  
51  
52  
53  
54  
55  
56  
57  
58  
59  
60

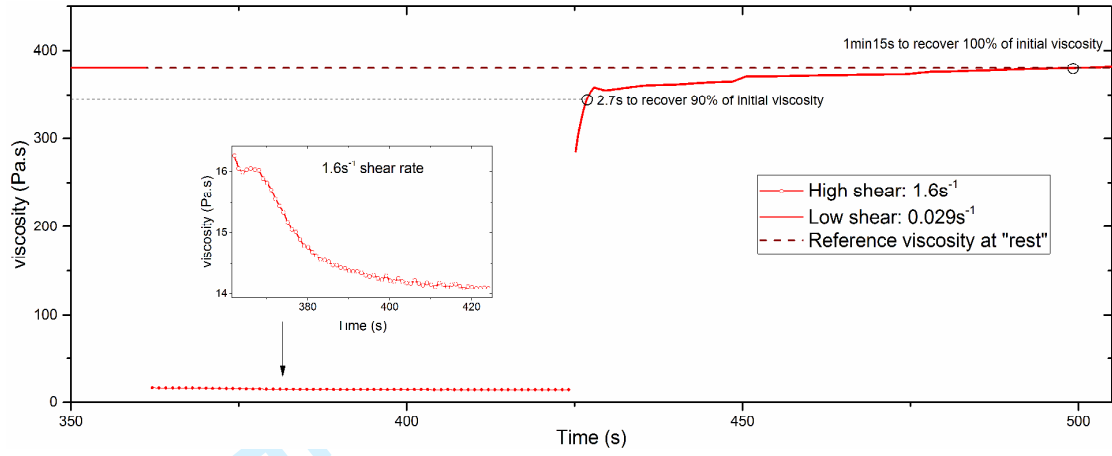


Figure 8

For Peer Review

1  
2  
3  
4  
5  
6  
7  
8  
9  
10  
11  
12  
13  
14  
15  
16  
17  
18  
19  
20  
21  
22  
23  
24  
25  
26  
27  
28  
29  
30  
31  
32  
33  
34  
35  
36  
37  
38  
39  
40  
41  
42  
43  
44  
45  
46  
47  
48  
49  
50  
51  
52  
53  
54  
55  
56  
57  
58  
59  
60

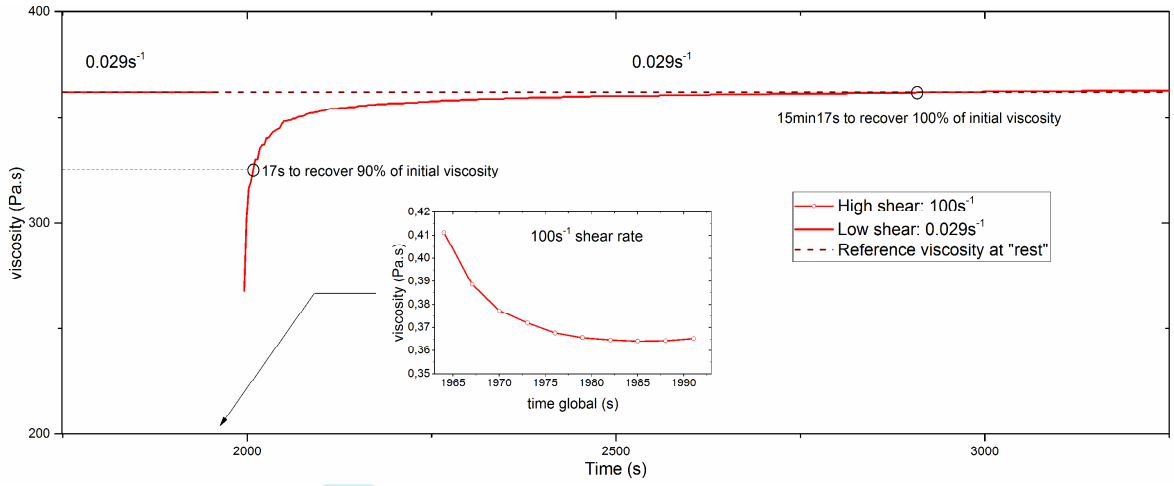


Figure 9

Peer Review

1  
2  
3  
4  
5  
6  
7  
8  
9  
10  
11  
12  
13  
14  
15  
16  
17  
18  
19  
20  
21  
22  
23  
24  
25  
26  
27  
28  
29  
30  
31  
32  
33  
34  
35  
36  
37  
38  
39  
40  
41  
42  
43  
44  
45  
46  
47  
48  
49  
50  
51  
52  
53  
54  
55  
56  
57  
58  
59  
60

**Table 1.** Evolution of limit stresses for LVE range,  $E_c$  and moduli plateau values vs active polymer concentrations.

[Actigum <sup>TM</sup> ](wt%)	$\tau_y$ (Pa)	$\tau_f$ (Pa)	$\tau_{peak}$ (Pa)	$E_c$ (J.m <sup>-3</sup> )	G' (Pa)	G'' (Pa)
0.50	0.32	1.55	-	0.024	2.07	0.88
0.75	0.63	2.88	2.37	0.035	5.52	2.02
1	1.96	4.92	5.02	0.073	26.56	6.06
1.50	4.15	9.20	9.32	0.143	61.18	12.34
2.00	6.98	15.00	14.78	0.360	67.64	14.66

For Peer Review

**Table 2.** Evolution of the HB model parameters vs. active polymer concentrations.

[Actigum <sup>TM</sup> ](wt%)	$\tau_{0HB}$ (Pa)	$K(\text{Pa}\cdot\text{s}^n)$	$n$
0.50	2.98	0.04	0.78
0.75	6.15	0.1	0.72
1	8.74	0.21	0.66
1.50	13.62	1.67	0.42
2.00	20.43	3.29	0.37

For Peer Review

1  
2  
3  
4  
5  
6  
7  
8  
9  
10  
11  
12  
13  
14  
15  
16  
17  
18  
19  
20  
21  
22  
23  
24  
25  
26  
27  
28  
29  
30  
31  
32  
33  
34  
35  
36  
37  
38  
39  
40  
41  
42  
43  
44  
45  
46  
47  
48  
49  
50  
51  
52  
53  
54  
55  
56  
57  
58  
59  
60